



Synthesis of aluminum-substituted tobermorite and the application on the phosphorus removal from waste water

Ling Li*, Zheng Xi Wu, Ya Xiong Li, Huai Li Sha, Gong Wu Song

Ministry of Education Key Laboratory for the Synthesis and Application of Organic Function Molecules, Hubei University, Wuhan, ROC

Tel. +86 2788662747; Fax: +86 2788663043; email: lingli_hubu@yahoo.cn

Received 6 March 2013; Accepted 28 April 2013

ABSTRACT

An Al-substituted tobermorite was prepared by hydrothermal treatment using 4A-zeolite, sodium silicate, and calcium hydroxide. The X-ray diffraction (XRD) patterns and FT-TR spectra confirmed that tobermorite was formed after the hydrothermal process. The removal of phosphorous using the synthesized tobermorite was studied. XRD patterns, FT-TR spectra, and scanning electron microscope (SEM) images showed the formation of hydroxyapatite after *p*-elimination. It was found that the best solid/liquid ratio is 1.0 g/L and the best pH value is 9. Kinetic models and thermodynamic parameters of *p*-elimination were discussed, and the *p*-elimination process was proved to follow pseudo-second-order rate kinetics; it was spontaneous and endothermic.

Keywords: Phosphorous remove; Tobermorite; P-elimination process

1. Introduction

Preparation of tobermorite has been attracting attention in recent years. Tobermorite, $\text{Ca}_5\text{Si}_6\text{O}_{16}(\text{OH})_2 \cdot 4\text{H}_2\text{O}$, is hydrated calcium silicate. It has a layer-type structure and is prepared using reactive Ca and Si as starting materials under hydrothermal conditions below 180 °C [1]. Tobermorite ($\text{Ca}_5\text{Si}_6\text{O}_{18}\text{H}_2 \cdot 4\text{H}_2\text{O}$) has been shown to have high potential applications in cation exchange, and nuclear and hazardous waste water treatment [2,3]. It is well known that the reactivity of silica source [4,5], addition of Al compounds [6,7], addition of alkali [8,9], and addition of sulfate compounds [1,10] strongly affect tobermorite formation.

Moreover, tobermorite was an effective adsorbent for the removal of phosphorous in waste water. In natural waters, phosphorus concentrations as low as 10 µg/L *P* can already lead to eutrophication processes and to the deterioration of the water quality. Because tobermorite can be easily and commercially synthesized, the water treatment system developed is rapid and simple, and it has potential for application in treatment of waste water, which could be adopted by developing nations.

Though most waste waters are supersaturated with respect to calcium phosphate compounds, spontaneous precipitation of calcium phosphate is kinetically inhibited. However, the supply of suitable seed material initiates the deposition of calcium phosphate compounds onto the seed material surfaces, in order

*Corresponding author.

to achieve equilibrium between Ca^{2+} and phosphate. OH^- and Ca^{2+} in Tobermorite, can form hydroxyapatite with phosphorus in waste water, resulting in the phosphorus elimination.

The goal of this study was to develop a simple technology for phosphorus elimination from waste water and the new material was proved apt to remove phosphorus.

2. Materials and methods

2.1. Materials and synthesis

The raw materials used for synthesis were $\text{Ca}(\text{OH})_2$, Na_2SiO_3 , and 4A-zeolite. All reagents were of analytical grade, made in China.

For the synthesis, distilled water (25 mL), $\text{Ca}(\text{OH})_2$, and Na_2SiO_3 were added to a Teflon reaction vessel. The synthetic conditions were set to give a CaO/SiO molar ratio of 0.83. The reaction vessel was put in an oven at 180°C for 10 h. The resulting product was washed thoroughly in distilled water and was dried at 100°C for 3 h.

The final sample was characterized by X-ray diffraction (XRD) and scanning electron microscope (SEM).

2.2. Phosphorus removal experiment

Simulated waste water containing 50 mg/L P was prepared by $\text{NaH}_2\text{PO}_4 \cdot \text{H}_2\text{O}$. 1.0 g/L synthesized tobermorite was added to 25 mL waste water, oscillated for an hour, after centrifugation the supernatant was measured to determine the concentration of phosphorus. The residue was dried and recycled, and added to 25 mL fresh waste water to remove phosphorus, so the Al-substituted tobermorite can be recycled to remove phosphorus repeatedly. The recycled Al-substituted tobermorite was characterized by XRD and SEM.

2.3. Apparatus

The absorbance at 700 nm was measured on a Perkin-Elmer lambda 17 UV-VIS spectrophotometer (P-E Co., America) with 10-mm cells for the determination of concentration of Phosphorus. SEM (Model EPMA-8705QH2, Shimadzu Co., Japan) was used to observe the morphologies of tobermorite. The crystalline structure and composition of the tobermorite were identified respectively by a D/max-IIIC X-ray diffractometer (Shimadzu, Japan). Fourier transform infrared (FTIR) spectra were taken with a Spectrum One FTIR spectrophotometer (Perkin-Elmer, America) at room temperature.

3. Results and discussion

3.1. Characterization of tobermorite

Fig. 1(a) shows the XRD patterns of the synthesized powder, prepared by the hydrothermal method. Numerous sharp peaks were observed in the XRD patterns and were identified as tobermorite [11]. The sharp diffraction peaks indicate that the tobermorite formed are well crystallized. Fig. 1(b) shows that after the recovery of phosphorus, the characteristic peaks of tobermorite become weak or disappear, and the peak position and intensity are similar with HAP [12], indicating that the phosphate existed as hydroxyapatite.

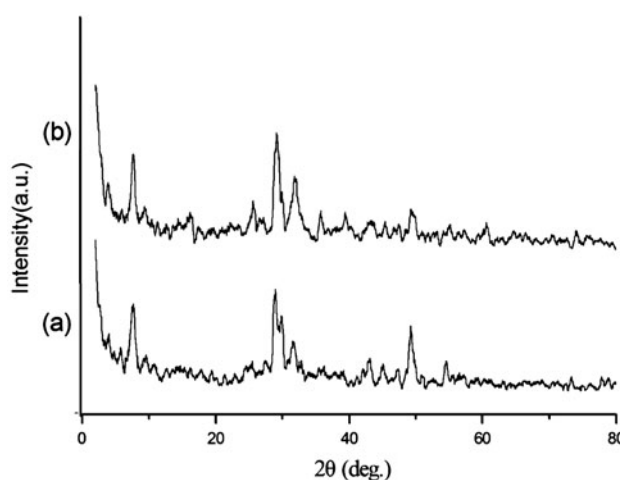


Fig. 1. XRD patterns of the as-synthesized powders. (a) synthesized tobermorite; (b) recycled tobermorite.

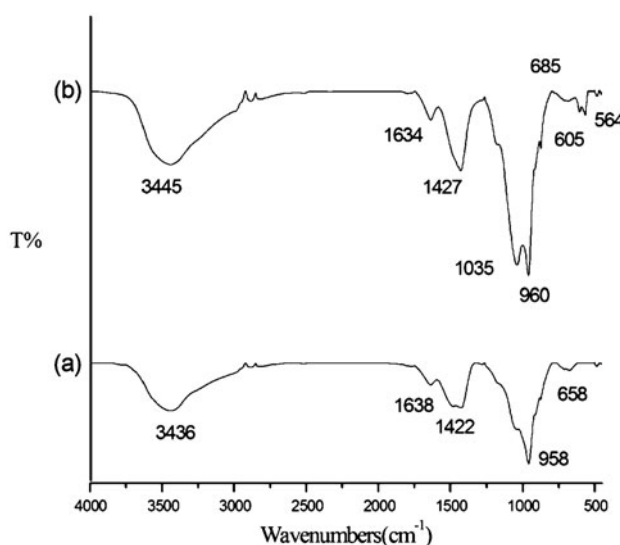


Fig. 2. FT-IR spectra of synthesized tobermorite and recycled tobermorite. (a) synthesized tobermorite; (b) recycled tobermorite.

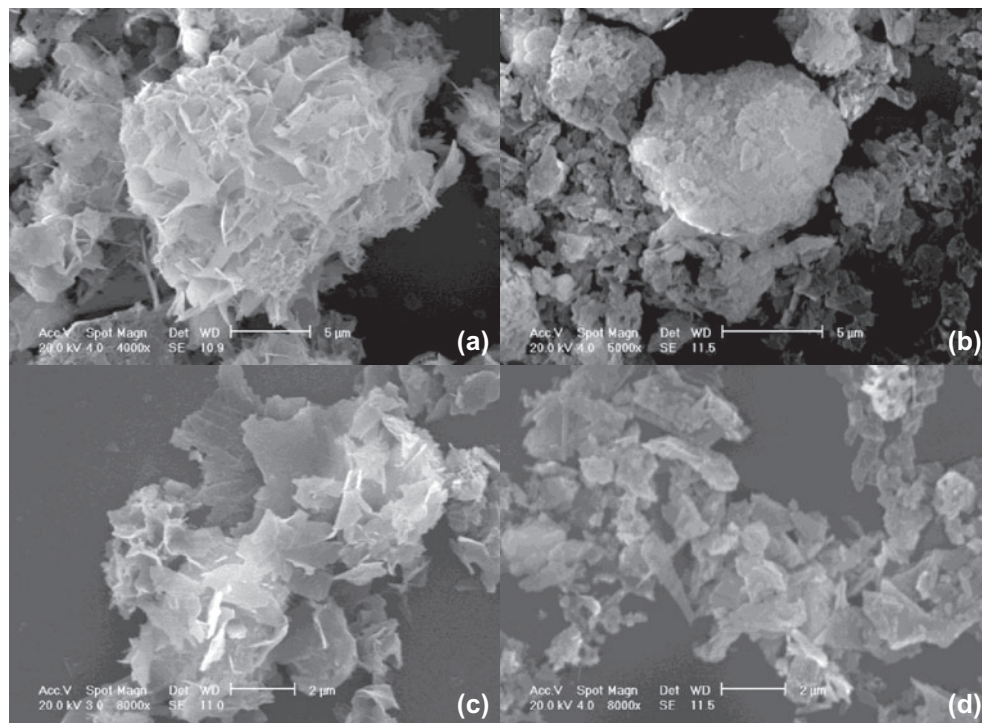


Fig. 3. SEM images of the synthesized and recycled tobermorite powders.

Fig. 2 shows the FT-TR spectra of synthesized tobermorite and recycled tobermorite. It can be seen from Fig. 2(a) that 3438 , 958 , and 658 cm^{-1} are characteristic peaks of tobermorite. Comparing with Fig. 2 (a), 1035 , 605 , and 564 cm^{-1} are characteristic peaks of PO_4^{3-} in Fig. 2(b), indicating that hydroxyapatite crystals are formed [12].

The surface morphology of tobermorite was analyzed by SEM. Typical results are shown in Fig. 3.

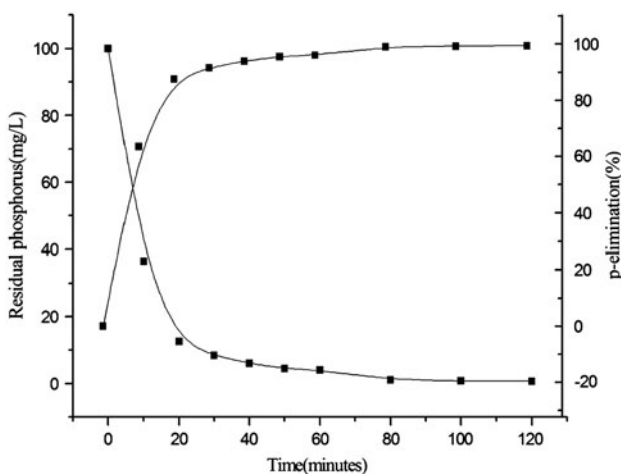


Fig. 4. Effect of the oscillate time on the phosphorous elimination efficiency.

Before adsorption of phosphorous, the fine thin plate-like crystals on the surface of tobermorite can be observed (Fig. 3(a) and (c)) [13]. However, after the adsorption, the plate-like form disappears (Fig. 3(b) and (d)). The surface is covered with white flakes, which can explain the hydroxyapatite formed [12].

3.2. Phosphorus removal by tobermorite

Fig. 4 shows the effect of oscillation time on the elimination efficiency. Simulated waste water is used in experiments and the concentration of P is 50 mg/L . The elimination efficiency is 96% over a period of about 1 h, indicating that the tobermorite has good phosphorous removal capacity. It can also be seen that the residual phosphorus content remained almost unchanged, when oscillation time was more than one hour. Therefore, one hour is selected as the optimal oscillation time in experiments.

Fig. 5 is the effect of the tobermorite amount on the phosphorous removal. It shows that when tobermorite amount (solid/liquid ratio) is 1.0, 1.5, or 2.0 g/L, the p-elimination efficiency is relative high and nearly kept a constant. However, when tobermorite amount is over than 2.0 g/L, p-elimination efficiency declines. It can be explained that with the increase in the amount of tobermorite, the concentration of dissolved Ca^{2+} and OH^- increases, thereby pH value increases,

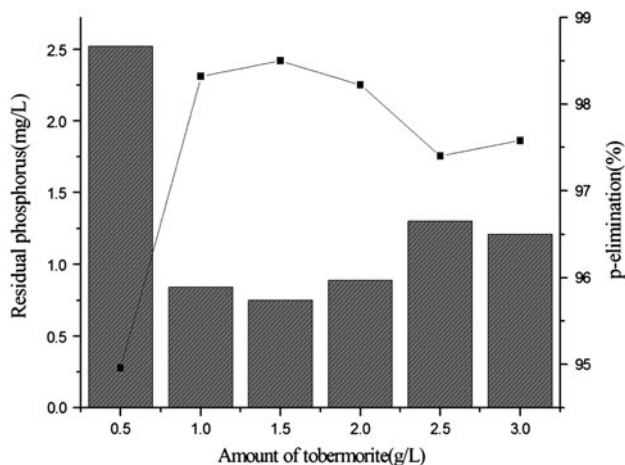


Fig. 5. Effect of the tobermorite amount on the phosphorous removal.

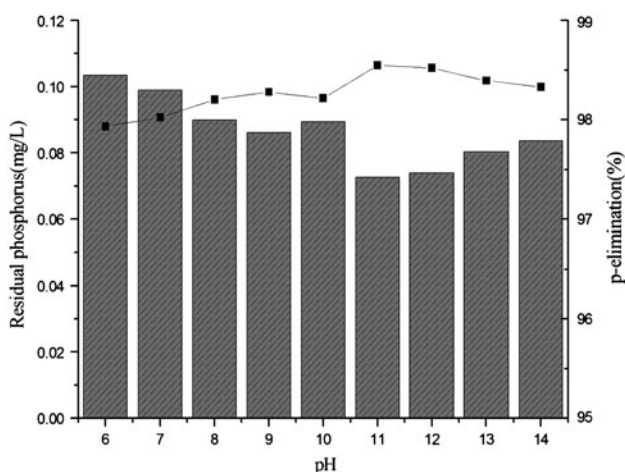


Fig. 6. The effect of pH value on the adsorption.

which is conducive to the generation of hydroxyapatite. The increase in Ca^{2+} concentration can increase super saturation, which is also conducive to crystallization. But when Ca^{2+} concentration increases to a certain extent, crystal nucleus formed by heterogeneous nucleation will be too much, and a large number of small crystal nuclei will form, which is difficult to separate from the liquid phase, so phosphorus removal rate declines.

3.3. The effect of pH value on the adsorption

The effect of pH value on the adsorption is shown in Fig. 6. It is clear that the *p*-elimination efficiency increases with increasing pH value, which can be explained that the increasing pH value is conducive to

the generation of hydroxyapatite. When pH value is beyond 9, the *p*-elimination efficiency is not stable, and the reason is probably that the formation of CaCO_3 has an effect on the formation of hydroxyapatite in a strong basic condition. Therefore, pH 9 is selected for experiments.

3.4. Kinetic models of *p*-elimination

The *p*-elimination model which describes the sorption of a solute onto a solid surface can be expressed in the following way:

$$\frac{dq}{dt} = k_1(q_e - q_t) \quad (1)$$

where k_1 is the apparent pseudo-first-order constant (in min^{-1}), q_t is the extent of sorption at time t (in mg g^{-1}), and q_e is the extent of sorption at equilibrium (in mg g^{-1}). This law is used to describe processes in which the reaction rate, dq_t/dt , is proportional to the number of available sorption sites, $(q_e - q_t)$. The linear, integrated form of this equation for the boundary conditions; $q_t = 0$ at $t = 0$ and $q_t = q_t$ at $t = t$, can be written as:

$$\ln(q_e - q_t) = \ln q_e - k_1 t \quad (2)$$

hence, the rate equation is obeyed when a linear relationship exists between $\log(q_e - q_t)$ and t , in which case k_1 may be estimated from the gradient of the plot. Similarly, the expression can be used to describe sorption processes in which the reaction rate is proportional to the square of the number of available sorption sites.

$$\frac{dq_t}{dt} = k_2(q_e - q_t)^2 \quad (3)$$

where k_2 is the apparent pseudo-second-order rate constant (in $\text{g mg}^{-1} \text{min}^{-1}$), and can be integrated and rearranged thus:

$$\frac{t}{q_t} = \frac{1}{k_2 q_e^2} + \frac{t}{q_e} \quad (4)$$

gradient of a linear plot of t/q_t against t .

The applicability of the pseudo-first- and pseudo-second-order kinetic models to *p*-elimination by tobermorite has been tested by fitting the experimental data, to the models by least-squares regression analysis (as shown in Figs. 7 and 8, respectively). The apparent pseudo-rate constants, k_1 and k_2 , integrated rate equations, and corresponding squares of the

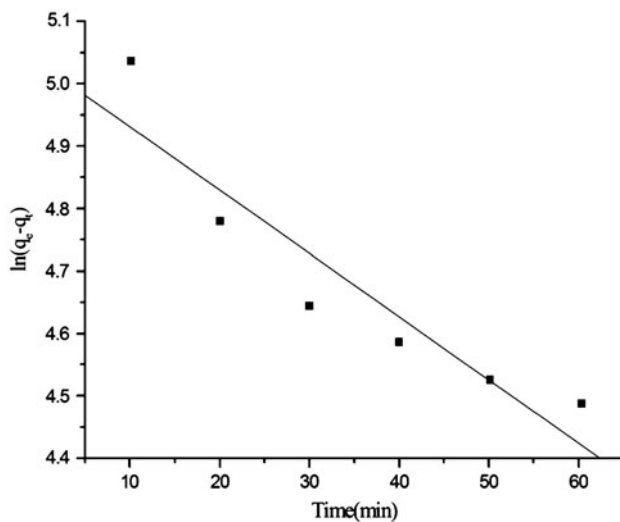


Fig. 7. Pseudo-first-order kinetic model fitted to experimental data for the p -elimination by tobermorite.

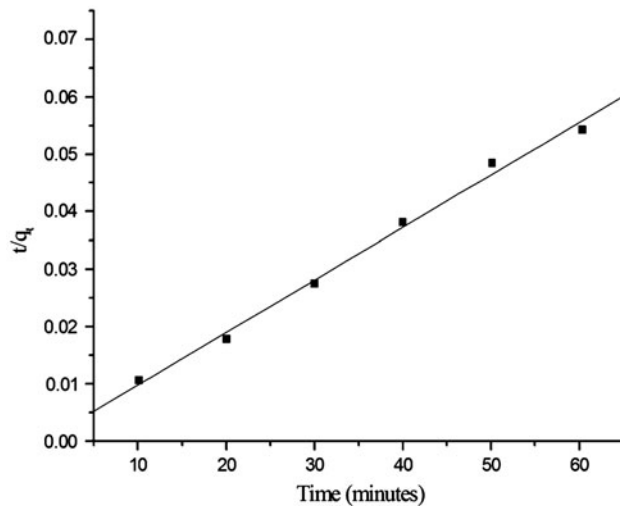


Fig. 8. Pseudo-second-order kinetic model fitted to experimental data for the p -elimination by tobermorite.

correlation coefficients, R^2 , are listed in Table 1. High correlations between the experimental data for the sorption of p by tobermorite and the pseudo-second-order kinetic model are indicated by R^2 values of 0.9970: whereas, R^2 values of 0.9328 were obtained by fitting the p -elimination data to the pseudo-first-order model and demonstrated that this model affords a less appropriate description of the sorption process.

3.5. Thermodynamic parameters of p -elimination

In the process of phosphorus adsorption, according to the adsorption equilibrium for different temperatures, the thermodynamic equilibrium constant (K) and the free energy change (ΔG) can be estimated from the following relationship:

$$K = \frac{q_e}{C_e} \quad (5)$$

$$\Delta G = -RT \ln K \quad (6)$$

If the enthalpy change (ΔH) does not vary significantly over the temperature range, its value and that of entropy change (ΔS) can be determined from the van't Hoff equation:

$$\ln K = -\frac{\Delta H}{RT} + \frac{\Delta S}{R}, \quad (7)$$

where K , ΔH , ΔS , and ΔG are obtained from the above equations and shown in Table 2. The negative free energy (ΔG) means that the phosphorus adsorption (p -elimination) is spontaneous. The positive enthalpy change (ΔH) means the process is an endothermic process, therefore, higher the temperature, greater the equilibrium constant. It indicates that phosphate adsorption of tobermorite becomes better with increasing temperature and thus the result of p -elimination will be better.

Table 1
Kinetic and statistical data for the pseudo-rate models

	Integrated rate equation	R^2
<i>Pseudo-first-order model</i>		
$k_1(\text{min}^{-1})$		
0.0101	$\ln(q_e - q_t) = -0.0101 t + 5.0324$	0.9328
<i>Pseudo-second-order model</i>		
$k_2(\text{g mg}^{-1} \text{min}^{-1})$		
0.00121	$t/q_t = 9.1426 \times 10^{-4} t + 6.9084 \times 10^{-4}$	0.9970

Table 2
Thermodynamic equilibrium constant K and relative thermodynamic parameters

T (K)	K	ΔH (kJ mol ⁻¹)	ΔS (J mol ⁻¹ K ⁻¹)	ΔG (kJ mol ⁻¹)
300	674.65	45.17	205.01	-16.33
310	1318.17			-18.38
316	1659.09			-19.61

4. Conclusion

A new one-step hydrothermal synthesis of Al-substituted tobermorite is reported, using 4A-Zeolite as reactants. The tobermorite product has been proved by XRD and FT-TR spectra. The p -elimination experiments are conducted by tobermorite. SEM images expose that hydroxyapatite is formed after p -elimination. The best oscillation time is one hour and the best tobermorite amount is 1.0 g.

The p -elimination process follows pseudo-second-order rate kinetics and the process is spontaneous. The positive enthalpy change (ΔH) means that the process is an endothermic process, indicating that the result of p -elimination becomes better with increasing temperature.

References

- [1] N.Y. Mostafa, A.A. Shaltout, H. Omarb, S.A. Abo-El-Enein, Hydrothermal synthesis and characterization of aluminium and sulfate substituted 1.1 nm tobermorites, *J. Alloys Compd.* 467 (2009) 332–337.
- [2] A. Zaoui, Insight into elastic behavior of calcium silicate hydrated oxide (C–S–H) under pressure and composition effect, *Cem. Concr. Res.* 42 (2012) 306–312.
- [3] K. Funasaka, K. Hatano, K. Ohta, Removal of natural organic polyelectrolytes by adsorption onto tobermorite, *Environ. Sci. Technol.* 37 (2003) 1448–1451.
- [4] C. Biagioni, E. Bonaccorsi, S. Merlino, D. Bersani, New data on the thermal behavior of 14 Å tobermorite, *Cem. Concr. Res.* 49 (2013) 48–54.
- [5] D.A. Kulik, Improving the structural consistency of C–S–H solid solution thermodynamic models, *Cem. Concr. Res.* 41 (2011) 477–495.
- [6] K. Matsui, J. Kikuma, M. Tsunashima, T. Ishikawa, S. Matsuno, A. Ogawa, M. Sato, In situ time-resolved X-ray diffraction of tobermorite formation in autoclaved aerated concrete: Influence of silica source reactivity and Al addition, *Cem. Concr. Res.* 41 (2011) 510–519.
- [7] M. Sakiyama, T. Maeshima, T. Mitsuda, Synthesis and crystal chemistry of Al substituted 11 Å tobermorite, *J. Soc. Inorg. Mater. Jpn.* 7 (2000) 413–419.
- [8] J. Reinik, I. Heinmaa, J. Mikkola, U. Kirso, Hydrothermal alkaline treatment of oil shale ash for synthesis of tobermorite, *Fuel* 86 (2007) 669–676.
- [9] R. Gabrovšek, B. Kurbus, D. Mueller, W. Wieker, Tobermorite formation in the system CaO, C₃S–SiO₂–Al₂O₃–NaOH–H₂O under hydrothermal conditions, *Cem. Concr. Res.* 23 (1993) 321–328.
- [10] K. Baltakys, Influence of gypsum additive on the formation of calcium silicate hydrates in mixtures with C/S=0.83 or 1.0, *Mater. Sci. Poland* 27 (2009) 1091–1101.
- [11] Y. Kojima, S. Kamei, T. Toyama, N. Nishimiya, Preparation of novel phosphor using intercalation of tobermorite, *J. Lumin.* 129 (2009) 751–754.
- [12] B.B. Zhang, H. Zheng, H.W. Ma, L.J. Han, H.M. Zhang, Phosphorus recovery from wastewater by synthetic tobermorite through seeded crystallization, *Acta Petrol. Mineral.* 26(6) (2007) 553–557.
- [13] X. Huang, D.L. Jiang, S.H. Tan, Novel hydrothermal synthesis of tobermorite fibers using Ca(II)–EDTA complex precursor, *J. Eur. Ceram. Soc.* 23 (2003) 123–126.